A charge density study of the intermetallic compound $MgCu_2$ by the maximum entropy method



2000 J. Phys.: Condens. Matter 12 1253

(http://iopscience.iop.org/0953-8984/12/7/309)

J. Phys.: Condens. Matter **12** (2000) 1253–1259. Printed in the UK PII: S0953-8984(00)04294-6

# A charge density study of the intermetallic compound $MgCu_2$ by the maximum entropy method

Y Kubota†, M Takata†‡, M Sakata†§, T Ohba†‖, K Kifune† and T Tadaki†

† Department of Environmental Sciences, Osaka Women's University, Sakai, Osaka 590-0035, Japan

‡ Department of Material Science, Shimane University, Matsue 690-8504, Japan

§ Department of Applied Physics, Nagoya University, Nagoya 464-8603, Japan

‖ Department of Materials Science and Engineering, Teikyo University, Utsunomiya 320-8551, Japan

Received 14 May 1999, in final form 5 October 1999

**Abstract.** The charge density distribution of the intermetallic compound $MgCu_2$ is obtained by the maximum entropy method (MEM) from the synchrotron powder diffraction data. In the MEM charge density map, the overlap of electron densities was clearly observed between the neighbouring Cu atoms. This clearly shows that there is a rather strong covalent bond between Cu–Cu atoms. It is also found that the Cu–Cu bonding is along the very well known kagome net, which characterizes the Laves phase structure. At least, in the case of $MgCu_2$, the kagomé network is the electronic network in reality rather than a geometrical concept to represent structural characteristics of Laves phase compounds.

## 1. Introduction

In the Laves phase compounds, there are three types of fundamental structure, $MgZn_2$ (2H), $MgCu_2$ (3C) and $MgNi_2$ (4H). They are considered as a layer structure and they have different stacking sequences. If we adopt a sphere-packing model, the ratio of the atomic radii of the constituent atoms is about 1.23 and the same kinds of atom are in contact with each other. The Laves phase has been considered as a typical size factor compound. Laves and Witte [1] and Komura and Kitano [2] systematically studied the crystal structures of the pseudo-binary systems of Mg-based Laves phases. They showed that the crystal structures are closely related to the electron concentration (e/a). This implies that the stability of the crystal structures is strongly governed by the valence state of the constituent atoms. Different bonding nature is expected for the different stacking sequences in the three types of fundamental structure. In order to see the differences, the charge density distribution of these compounds should be studied. There are some theoretical studies on the factors governing the stability of the Laves phase structures [3–7], but the charge density studies are very few [8, 9]. Ohba *et al* [9] obtained the structure factors of $MgZn_2$ and $MgCu_2$ by the single crystal x-ray diffraction method. They showed that the charge transfers occurred between the constituent atoms by the population analysis and the localized electrons were seen in the centre of the tetrahedra formed by the small atoms in the difference Fourier maps. But the distinct differences of the bonding nature related to the different stacking sequences were not found.

In recent years, a maximum entropy method (MEM) [10] has been widely used in crystallography, for example, for a phase problem [11, 12], and accurate charge and spin

0953-8984/00/071253+07$30.00  

density studies [13, 14]. In the accurate charge density studies, it can directly obtain the high-resolution charge density distributions from the x-ray diffraction data without any structure models. This is a very powerful method to visualize the features of a chemical bond in real space. In recent years, the MEM has been applied to the accurate structure analysis of many kinds of material, e.g., Si [15, 16], $CeO_2$ [17], ice ($I_h$) [18], $TiO_2$ [19], $h$-BN [20] etc. Recently, it was successfully applied to the structure analysis for fullerene compounds [21, 22]. In the case of metals, a few hexagonal close-packed simple metals were studied such as Be [23] and Mg [24] by the MEM. In the MEM charge density maps of both simple metals, the localized electrons were observed in the space around the tetrahedral holes. These electrons connect the atoms within the basal plane of a hexagonal close-packed structure and form a honeycomb-shaped electronic network. Such a feature of the bonding can be explained to be due to the $sp^2$ hybridization. Then it was concluded that these elements have an electronic layer structure. This may be an example that there exists a kind of chemical bond nature, which cannot be explained by a simple model like a nearly free electron model even in simple metals. In the case of intermetallic compounds, there is a possibility that localized electron densities due to the hybrid orbitals can be expected to be observed together with widespread nearly free electrons. The MEM enables us to observe such a feature of bonding.

In the present study, a charge density distribution of the intermetallic compound $MgCu_2$, which is also one of the Laves phase compounds, is obtained from the synchrotron powder diffraction data by the MEM. This is the first step to reveal the differences of bonding nature in three types of fundamental structure of the Laves phase compounds.

## 2. Experiment

A bulk specimen of $MgCu_2$ was prepared by melting together Mg and Cu in an argon-filled induction furnace. The melt in a graphite crucible was vigorously stirred and then cast into a cylindrical steel mould. The purity of materials used was 99.9% for Mg and 99.999% for Cu, respectively. The x-ray powder samples were prepared by crushing the ingot. The granularity of the powder was made even less than $\sim$3 micron diameter by the precipitation method in order to obtain a homogeneous intensity distribution in the Debye–Scherrer powder ring.

In order to have a physically meaningful MEM charge density distribution, it is very important to obtain the reliable structure factors, because the MEM derives a charge density distribution to be consistent with the experimental data within the errors without using any structure models. In the x-ray single crystal diffraction method, lower angle reflections tend to be affected by the extinction effect and must be corrected by a method which has to depend on the structure model. In this study, the powder diffraction method was adopted to collect x-ray diffraction data in order to avoid the extinction correction. To have better resolution, the synchrotron powder x-ray diffraction data were measured by the high-resolution powder diffractometer with the multiple detector system [25] at the beam line BL-$4B_2$ at the Photon Factory. The specimen holder was kept rotating in the plane of the sample surface at 1 Hz for the whole measurement time. Ge(111) flat crystals were used for the analyser of each arm. The wavelength of the incident x-rays was 0.9 Å. The data were collected by asymmetric $2\theta$ scan with an incident angle fixed at 7 degrees at room temperature. The step interval was 0.004 degrees. The fixed counting time at each step was 3 s for $MgCu_2$. The highest count of the powder pattern was about 31 000 counts, which represents the goodness of counting statistics for the present data.

## 3. Data analysis

The charge density distribution was obtained by the MEM combined with the Rietveld analysis [21, 26, 27]. The procedure of the MEM/Rietveld analysis is shown in [27] in detail. In the preliminary Rietveld refinement, the observed intensities were analysed based on the C15-type structure of $MgCu_2$, which is shown in figure 1. The crystal data and structural parameters refined by the Rietveld analysis are shown in table 1 and the fitting result of the Rietveld refinement for $MgCu_2$ is shown in figure 2. There were no significant amounts of impurity phase and all reflections were indexed as an $MgCu_2$ single phase. The full width at half maximum was 0.023 degrees for the 111 reflection. The reliable factor based on the Bragg intensities, $R_I$ was 4.6% and the weighted profile $R$ factor, $R_{WP}$ was 14.1%. The reflections up to 0.98 $Å^{-1}$ in $\sin\theta/\lambda$ were used in the Rietveld refinement. Observed structure factors were evaluated according to the calculated contribution of individual reflections by a modified Rietveld refinement program. Eventually 79 observed structure factors were derived by the preliminary Rietveld refinement. The phase of the structure factors are calculated as C15-type structure. It can be safely said that there are no misassignments of the phases. Finally, the

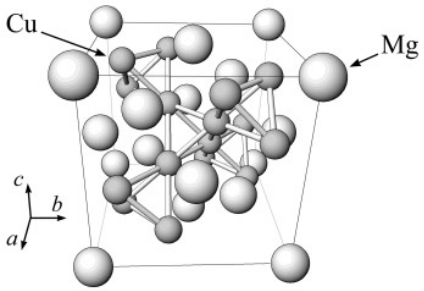


**Figure 1.** The crystal structure of $MgCu_2$.

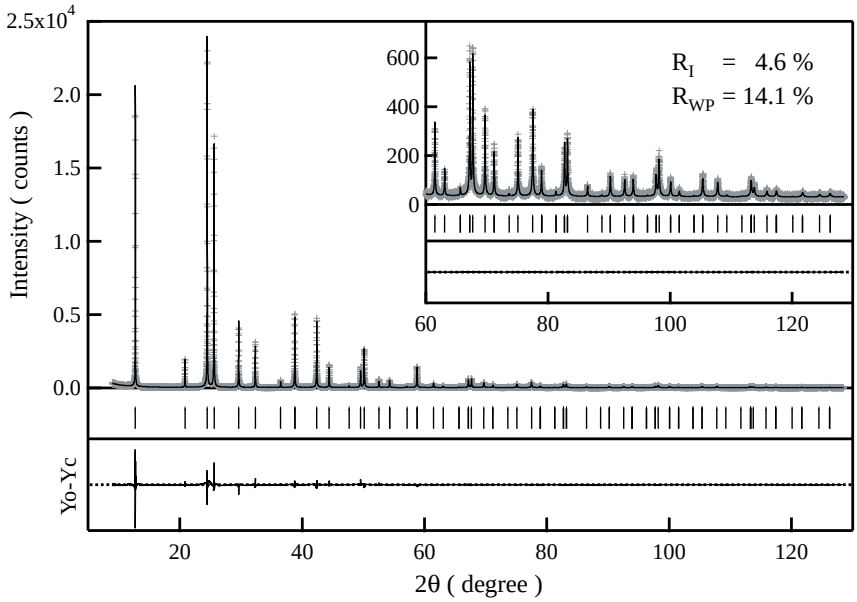


**Figure 2.** The fitting result of the Rietveld analysis for $MgCu_2$.

**Table 1.** The crystal data and structural parameters for $MgCu_2$ refined by the Rietveld analysis.

| Space group | $Fd\bar{3}m$ | | | | |
|---|---|---|---|---|---|
| Lattice parameter | $a = 7.035\,25\ (1)$ Å | | | | |
| Atom | Site | $x$ | $y$ | $z$ | $B$ [Å$^2$] |
| Mg | 8a | 1/8 | 1/8 | 1/8 | 0.78 (2) |
| Cu | 16d | 1/2 | 1/2 | 1/2 | 0.82 (1) |

$R_I = 4.6\%$ $R_{WP} = 14.1\%$.

MEM analysis was carried out by the computer program MEED [28] with the 79 structure factors. In the MEED calculation, the unit cell was divided into $144 \times 144 \times 144$ pixels. In this study, Collins' formalism [29] was employed and an uniform density distribution was used as the prior distribution.

## 4. MEM charge density distribution of $MgCu_2$

The MEM charge density maps of the (110) plane for $MgCu_2$ are shown in figure 3. In $MgCu_2$ structure, Mg atoms form a diamond type lattice and Cu tetrahedra are situated in the space among the Mg atoms. The (110) plane is bisecting the Cu tetrahedra. Figure 3(a) shows the higher density region of the plane, which corresponds to the core electron distribution of Mg and Cu atoms. Mg atoms have almost spherical distribution, while Cu atoms are slightly deformed. Figure 3(b) shows the lower density region of the same plane. The contour lines of the higher density regions are omitted. The equi-density regions are shaded according to the electron density, the darker the lower of the electron density. In figure 3(b), the rather clear overlap of electron densities showing the existence of covalent bonds is recognized between the neighbouring Cu atoms. This is probably due to the hybridization of the atomic orbitals of Cu atoms. The height of the charge density at the bond midpoint is 0.51 e Å$^{-3}$. This value is rather high as the charge density of the interatomic region of metals. Incidentally, the charge density of the bond midpoint of a typical covalent crystal Si is 0.61 e Å$^{-3}$ [16]. Therefore, it can be said that the hybridization is very significant in $MgCu_2$. In contrast to the Cu–Cu bonding, no overlap of electron densities is seen around the Mg atom. In the interatomic region, the electrons distribute evenly like a metallic bond whose nature is well explained by the nearly free electron model. The height of the charge density in the interatomic region is 0.19 e Å$^{-3}$.

One of the structural characteristics of the Laves phase compounds is the well known kagome net [30, 31]. If the cubic $MgCu_2$ structure can be considered as a stacking layer structure in terms of the hexagonal axis, one of the stacking layers is a denser layer forming the kagome net. The kagome net is composed of regular triangles and hexagons of Cu atoms. The Cu triangle corresponds to the base of the Cu tetrahedron and Mg atoms are situated above and below the hexagon. The kagome net plane is the {111} plane of the cubic $MgCu_2$ structure. It is very interesting to examine the charge density distribution of the kagome net. The MEM map of the kagome net plane is shown in figure 4. Only the lower density region is shown in this figure. It is very clearly understood that the kagome net physically corresponds to the Cu–Cu covalent bonds. The present results show that the kagome net is not only a representation of the geometrical relations of Cu atoms but also it corresponds to the actual covalent bonds of Cu atoms. The bonding exists along the edge of Cu tetrahedra.

In $MgCu_2$ structure, kagome nets are crossing each other with a cubic symmetry and they form a tetrahedral connection of Cu atoms. In order to visualize the three-dimensional aspect of the bonding, an equi-contour surface of the MEM charge density distribution of

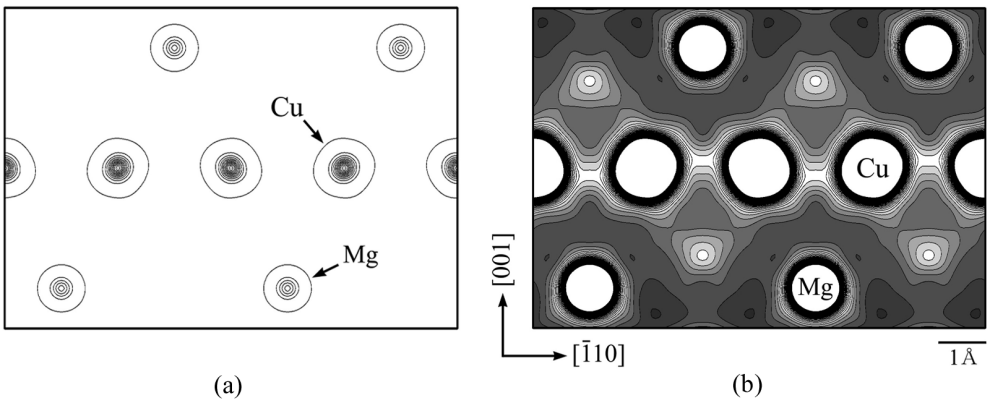


**Figure 3.** The MEM charge density distribution maps of the $MgCu_2$(110) plane. The contour lines are drawn (a) from 2.0 to 364.0 e Å$^{-3}$ with 30.0 e Å$^{-3}$ intervals and (b) from 0.0 to 2.0 e Å$^{-3}$ with 0.05 e Å$^{-3}$ intervals.

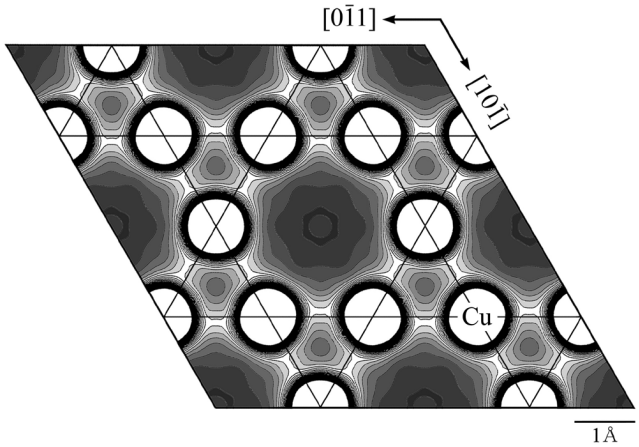


**Figure 4.** The MEM charge density distribution map of the kagome net plane for $MgCu_2$. The kagome net plane corresponds to the {111} plane of cubic $MgCu_2$ structure. The contour lines are drawn from 0.0 to 2.0 e Å$^{-3}$ with 0.05 e Å$^{-3}$ intervals. The lines connecting atomic sites show the kagome network.

$MgCu_2$ is shown in figure 5. In order to prevent the complication of the map, only the Cu network in a unit cell is shown. The equi-contour level is 0.45 e Å$^{-3}$. Figure 5 shows that the Cu–Cu bonding forms a three-dimensional tetrahedral electronic network. Mg atoms, which are not drawn in this map, are situated in the hole made by the tetrahedral Cu network. All Cu atoms are crystallographically equivalent. The bondings probably due to the hybrid of atomic orbitals extend from the Cu atom along the edge of Cu tetrahedra and form a trigonal antiprism structure. The possibility of such hybrids with six lobes is suggested by Altmann *et al* [32] from the geometrical consideration of the relation between the bond hybrids and metal structures. They proposed that such a bonding feature is explained by the $p^3d^3$ hybrids and a basic structure of the $p^3d^3$ hybrids gives a face-centred cubic structure. The Cu tetrahedra in the $MgCu_2$ structure are based on a face-centred cubic structure. It seems that the present MEM map shows the existence of the $p^3d^3$ hybridization.

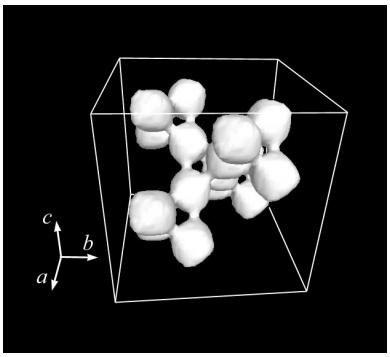


**Figure 5.** The MEM charge density distribution map of the Cu network for $MgCu_2$ by an equi-contour surface. Mg atoms are not drawn in this figure. The equi-contour level is 0.45 e $Å^{-3}$.

In figures 3(b) and 4, it is also recognized that the covalent bond between Cu–Cu atoms is slightly shifted from the centreline of Cu–Cu sites toward the Mg atom. In the Si case [16], the bonding electrons distribute symmetrically along the centreline of adjacent atoms. In the case of $MgCu_2$, the distribution of bonding electrons has a slightly different feature. The core density distribution of Cu atoms is also slightly deformed in the direction of the shifted bonding (see figure 3(a)). Since the MEM analysis is performed for the total charge density, the valence of each atom can be estimated by the summation of the number of electrons around the atomic site. From the MEM charge density of $MgCu_2$, the valence of the Mg atom is estimated to be about +2. Therefore there may be an ionic interaction between the hybridized orbital and the positively charged Mg ions.

Hafner [8] theoretically studied the charge densities for several simple metal Laves phases by the pseudopotential calculation. Though the charge density of $MgCu_2$ was not calculated, the valence density maps of $CaAl_2$ that has the same structure (C15-type structure) as $MgCu_2$ was shown in his paper. The overlap of electron densities showing the covalency is seen between the small atoms (Al atoms). The shift of bonding is also recognized in $CaAl_2$, but the direction of shift is opposite to that of $MgCu_2$. Since the small atom Al in $CaAl_2$ has the s and p type valence electrons only and the Cu have 3d electrons in addition, the bonding features cannot be simply compared. Nonetheless it is worthwhile to point out the coincidence of the nature of the chemical bond of experimental and theoretical works found in these Laves phase compounds. This suggests that the covalent bond between the small atoms along the kagome net may be a common feature in the charge densities of the C15-type Laves phases. Hafner also noted that he did not apply the pseudopotential calculation to $MgCu_2$ for the reason that the hybridization of the valence electrons with 3d electrons cannot be neglected. This seems consistent with the present results.

## 5. Conclusions

The charge density distribution of the intermetallic compound $MgCu_2$ was obtained from the synchrotron powder diffraction data by the MEM. It was found from the MEM charge density map that there exist strong covalent bonds between the Cu atoms. The bonding is along the kagome net and forms a tetrahedral electronic network in $MgCu_2$ structure. From the geometrical consideration, such a characteristic feature of bonding can be interpreted as the existence of the $p^3d^3$ hybridization. On the other hand, there is virtually no covalency between Cu and Mg atoms, although $MgCu_2$ are called intermetallic compounds. In the interatomic region, the electrons are distributed evenly like a metallic bond.

The present work revealed the nature of chemical bond of one of the three types of fundamental Laves phase structure. It is now highly desirable to study the other fundamental Laves phase structures, $MgZn_2$ and $MgNi_2$ by the same technique as used in this work.

## Acknowledgments

The authors thank Professor H Toraya of the Ceramics Research Laboratory of Nagoya Institute of Technology and Professor K Ohsumi of the Photon Factory for their kind help and suggestions in data collection. We also thank Professor H Tanaka of Shimane University for valuable discussions. This work was financially supported by a Grant-in-Aid for Scientific Research from the Ministry of Education, Science and Culture of Japan, the TARA Sakabe Project, the Japanese Atomic Energy Research Institute, the Murata Science Foundation and the Sumitomo Foundation to which the authors' thanks are due. This work has been performed under the approval of the Photon Factory Program Advisory Committee and the SPring-8 Proposal Review Committee.

## References

[1] Laves F and Witte H 1936 *Metallwirtschaft* **15** 840–2
[2] Komura Y and Kitano Y 1977 *Acta Crystallogr.* B **33** 2496–501
[3] Berry R L and Raynor G V 1953 *Acta Crystallogr.* **6** 178–86
[4] Elliott R P and Rostoker W 1958 *Trans. AMS* **50** 617–33
[5] Dwight 1961 *Trans. AMS* **53** 479–500
[6] Haydock R and Johannes R L 1975 *J. Phys. F: Met. Phys.* **5** 2055–67
[7] Rennert P and Radwan A M 1977 *Phys. Status Solidi* b **79** 167–73
[8] Hafner J 1985 *J. Phys. F: Met. Phys.* **15** 1879–93
[9] Ohba T, Kitano Y and Komura Y 1984 *Acta Crystallogr.* C **40** 1–5
[10] Gilmore C J 1996 *Acta Crystallogr.* A **52** 561–89
[11] Bricogne G 1991 *Acta Crystallogr.* A **47** 803–29
[12] Gilmore C J, Henderson K and Bricogne G 1991 *Acta Crystallogr.* A **47** 830–41
[13] Papoular R J, Zheludev A, Ressouche E and Schweizer J 1995 *Acta Crystallogr.* A **51** 295–300
[14] Papoular R J, Vekhter Y and Coppens P 1996 *Acta Crystallogr.* A **52** 397–407
[15] Sakata M and Sato M 1990 *Acta Crystallogr.* A **46** 263–70
[16] Takata M and Sakata M 1996 *Acta Crystallogr.* A **52** 287–90
[17] Sakata M, Mori R, Kumazawa S, Takata M and Toraya H 1990 *J. Appl. Crystallogr.* **23** 526–34
[18] Sakata M, Takata M, Oshizumi H, Goto A and Hondo T 1992 *Physics and Chemistry of Ice* (New York: Plenum) pp 62–8
[19] Sakata M, Uno T, Takata M and Mori R 1992 *Acta Crystallogr.* B **48** 591–8
[20] Yamamura S, Takata M and Sakata M 1997 *J. Phys. Chem. Solids* **58** 177–83
[21] Takata M, Umeda B, Nishibori E, Sakata M, Saito Y, Ohno M and Shinohara H 1995 *Nature* **377** 46–9
[22] Takata M, Nishibori E, Umeda B, Sakata M, Yamamoto E and Shinohara H 1997 *Phys. Rev. Lett.* **78** 3330–3
[23] Takata M, Kubota Y and Sakata M 1993 *Z. Naturf.* a **48** 75–80
[24] Kubota Y, Takata M and Sakata M 1993 *J. Phys.: Condens. Matter* **5** 8245–54
[25] Toraya H, Hibino H and Ohsumi K 1996 *J. Synchrotron Radiat.* **3** 75–83
[26] Hasegawa K, Nishibori E, Takata M, Sakata M, Togashi N, Yu J and Terasaki O 1999 *Japan. J. Appl. Phys. Suppl.* **38-1** 65–8
[27] Takata M, Machida N, Nishibori E, Umeda B, Sakata M, Tanigaki K, Kosaka M, Hirosawa I and Mizuki J 1999 *Japan. J. Appl. Phys. Suppl.* **38-1** 122–5
[28] Kumazawa S, Kubota Y, Takata M, Sakata M and Ishibashi Y 1993 *J. Appl. Crystallogr.* **26** 453–7
[29] Collins D M 1982 *Nature* **298** 49–51
[30] Frank F C and Kasper J S 1958 *Acta Crystallogr.* **11** 184–90
[31] Frank F C and Kasper J S 1959 *Acta Crystallogr.* **12** 483–99
[32] Altmann S L, Coulson C A and Hume-Rothery W 1957 *Proc. R. Soc.* A **240** 145–59